

SUPPLEMENTARY MATERIAL

A comprehensive investigation of the $(\text{Ti}_{0.5}\text{Zr}_{0.5})_1(\text{Fe}_{0.33}\text{Mn}_{0.33}\text{Cr}_{0.33})_2$ multicomponent alloy for room-temperature hydrogen storage designed by computational thermodynamic tools

Jéssica Bruna Ponsoni^{a,b}, Mateusz Balcerzak^{*b,c}, Walter José Botta^{a,d}, Michael Felderhoff^b, Guilherme Zepon^{*a,d}

- a. Graduate Program in Materials Science and Engineering (PPGCEM/UFSCar) - Rodovia Washington Luiz, km 235, Federal University of Sao Carlos, São Carlos, São Paulo CEP: 13565-905, Brazil
- b. Department of Heterogeneous Catalysis, Max-Planck-Institut für Kohlenforschung, Kaiser-Wilhelm Platz 1, Mülheim an der Ruhr, 45470, Germany
- c. Institute of Materials Science and Engineering, Poznan University of Technology, Jana Pawła II No 24, Poznan 61-138 Poland
- d. Department of Materials Engineering (DEMa/UFSCar) - Rodovia Washington Luiz, km 235, Federal University of São Carlos, São Carlos CEP: 13565-905, Brazil

*Corresponding authors: balcerzak@kofo.mpg.de, zepon@ufscar.br

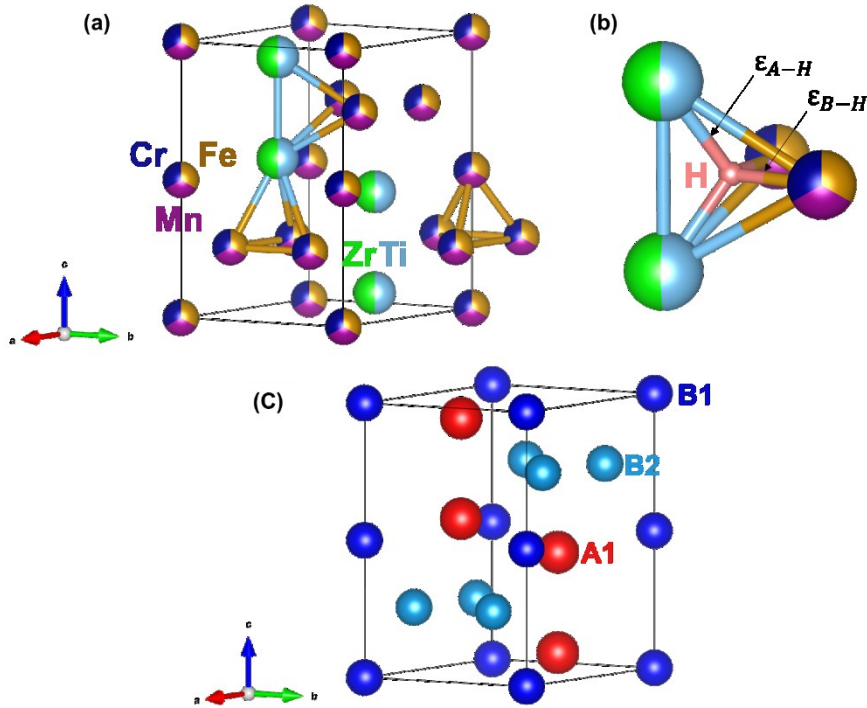


Fig. S1. (a) Unit cell of the hexagonal C14 Laves phase (MgZn₂-type). The three types of tetrahedral interstices available are A₂B₂, AB₃, and B₄. (b) A₂B₂ sites are formed by a tetrahedron having two bonds with energy ε_{A-H} and two bonds with energy ε_{B-H}. (c) Unit cell showing the Wyckoff position: 4f (A1), 2a (B1), and 6h (B2) positions. The red spheres represent the A1 positions, and the blue spheres represent the B positions (B positions are divided into two different crystallographic positions: B1 = dark blue and B2 = light blue).

Table S1. Crystal structure of C14 Laves phase in the (Ti_{0.5}Zr_{0.5})₁(Fe_{0.33}Mn_{0.33}Cr_{0.33})₂ alloy.

Phase	Sublattices	Wyckoff position	Element	Occupation factor ^b
C14 P6₃/mmc (194)	A1	4f ($\frac{1}{3}, \frac{2}{3}, z$) ^a	Ti	1/2
			Zr	1/2
	B1	2a (0, 0, 0)	Fe	1/3
			Mn	1/3
			Cr	1/3
	B2	6h ($x, 2x, \frac{1}{4}$) ^a	Fe	1/3
			Mn	1/3
			Cr	1/3

^a Fraction coordinates z of position 4f, and x, y of position 6h was considered the same as that of the ZrCr₂ Laves phase, i.e., 0.064, 0.835, and 0.67, respectively.

^b Occupation factor was calculated using the equiatomic composition.

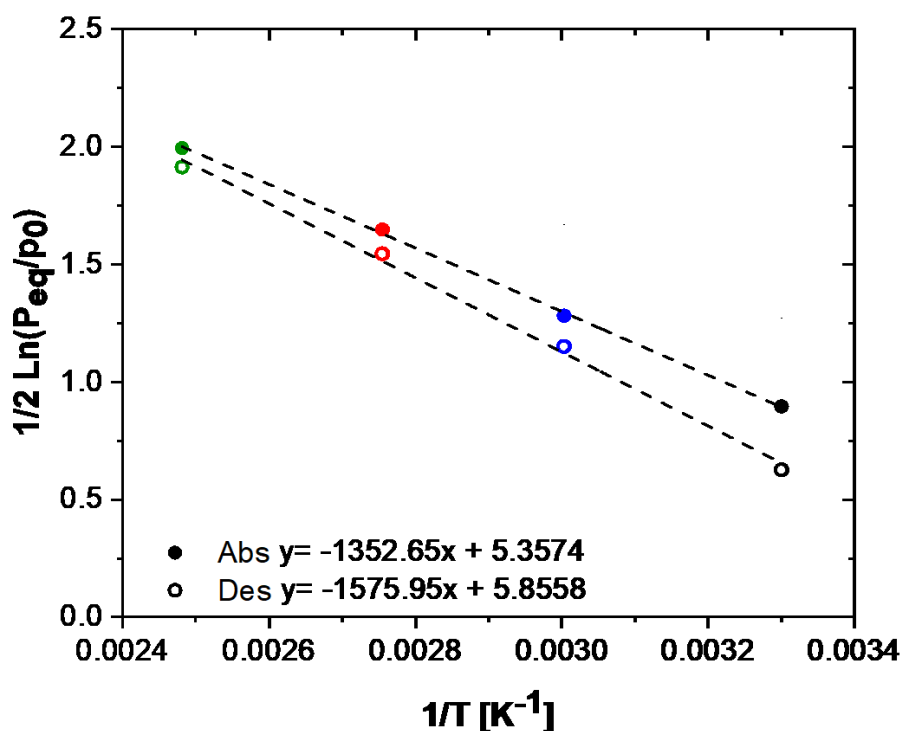


Fig. S2. Van't Hoff plot for the absorption and desorption pressure at $c_H = H/M = 0.5$.

Table S2. Thermodynamic data determined by van't Hoff analyses in absorption and desorption from the experimental PCI curves. The values of enthalpy and entropy are given in kJ/mol of H and J/K.mol of H, respectively, and correspond to a hydrogen concentration equal to $c_H = H/M = 0.5$.

Enthalpy [kJ/mol H]		Entropy [J/K.mol H]	
Absorption	Desorption	Absorption	Desorption
-11.246	-13.102	0.045	0.049

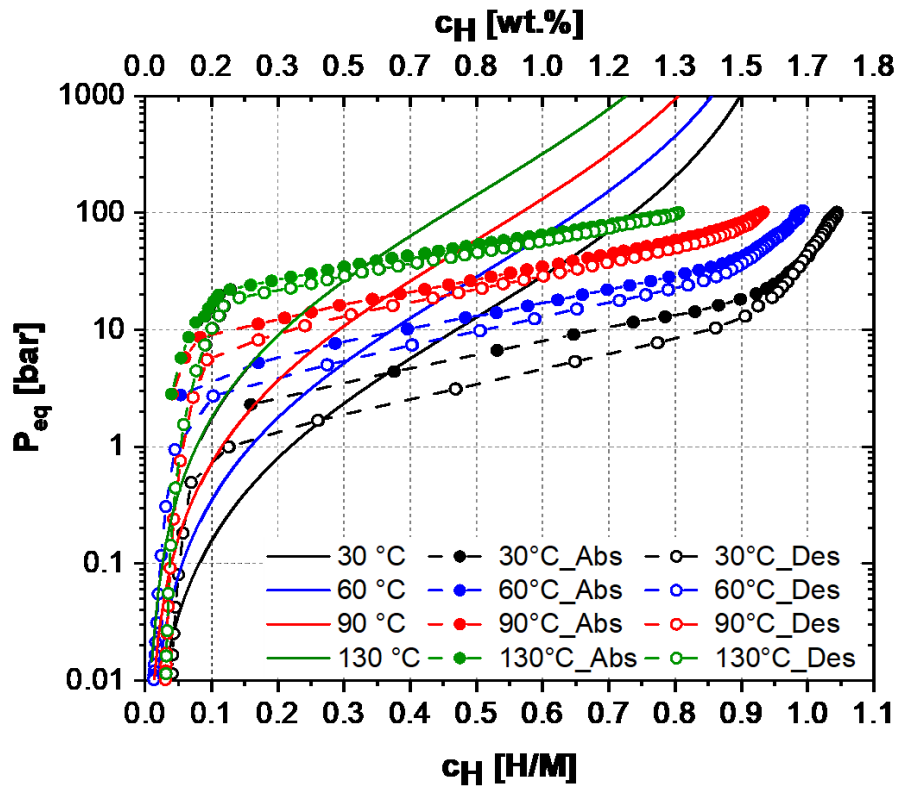


Fig. S3. Experimental PCIs of $(\text{Ti}_{0.5}\text{Zr}_{0.5})_1(\text{Fe}_{0.33}\text{Mn}_{0.33}\text{Cr}_{0.33})_2$ alloy at 30 °C, 60 °C, 90 °C and 130 °C (dash lines) compared with the calculated PCIs at the same temperatures (solid lines).

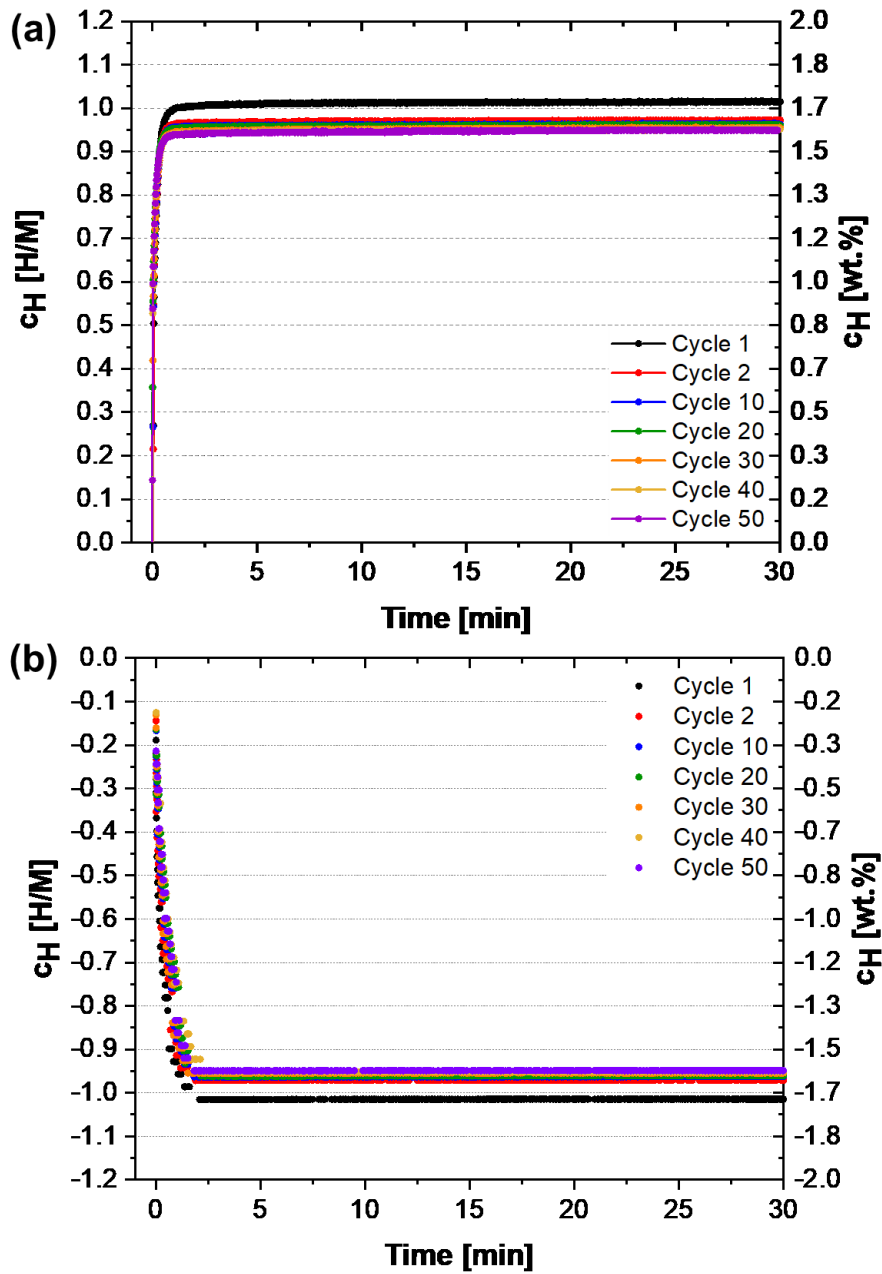


Fig. S4. Measurement of hydrogen (a) absorption and (b) desorption kinetics at 30 °C in H/M and wt.% of the $(\text{Ti}_{0.5}\text{Zr}_{0.5})_1(\text{Fe}_{0.33}\text{Mn}_{0.33}\text{Cr}_{0.33})_2$ alloy under an initial hydrogen pressure of 52 bar. At the end of the absorption measurement, the hydrogen pressure was 48 bar, and during desorption, 0.7 bar, approximately.

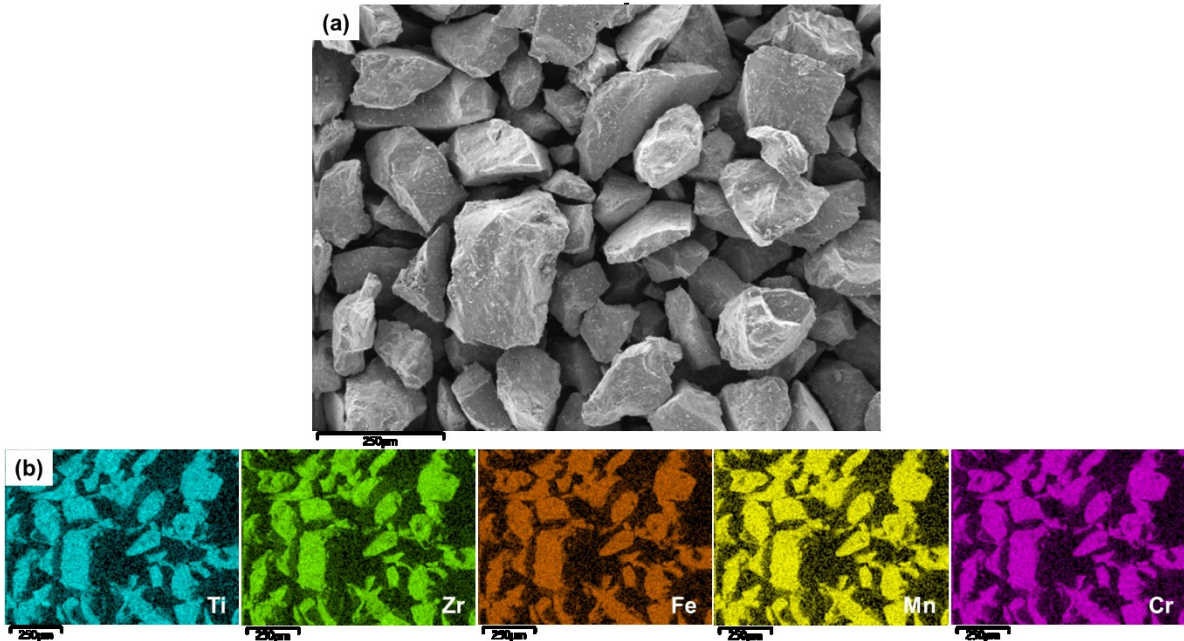


Fig. S5. SEM image and corresponding EDX elemental mappings of the as-cast $(\text{Ti}_{0.5}\text{Zr}_{0.5})_1(\text{Fe}_{0.33}\text{Mn}_{0.33}\text{Cr}_{0.33})_2$ alloy in the powder state. a) SEM images using the Back-Scattered Electrons (BSE) and b) EDX elemental mappings with selected elements: Ti, Zr, Fe, Mn, and Cr.

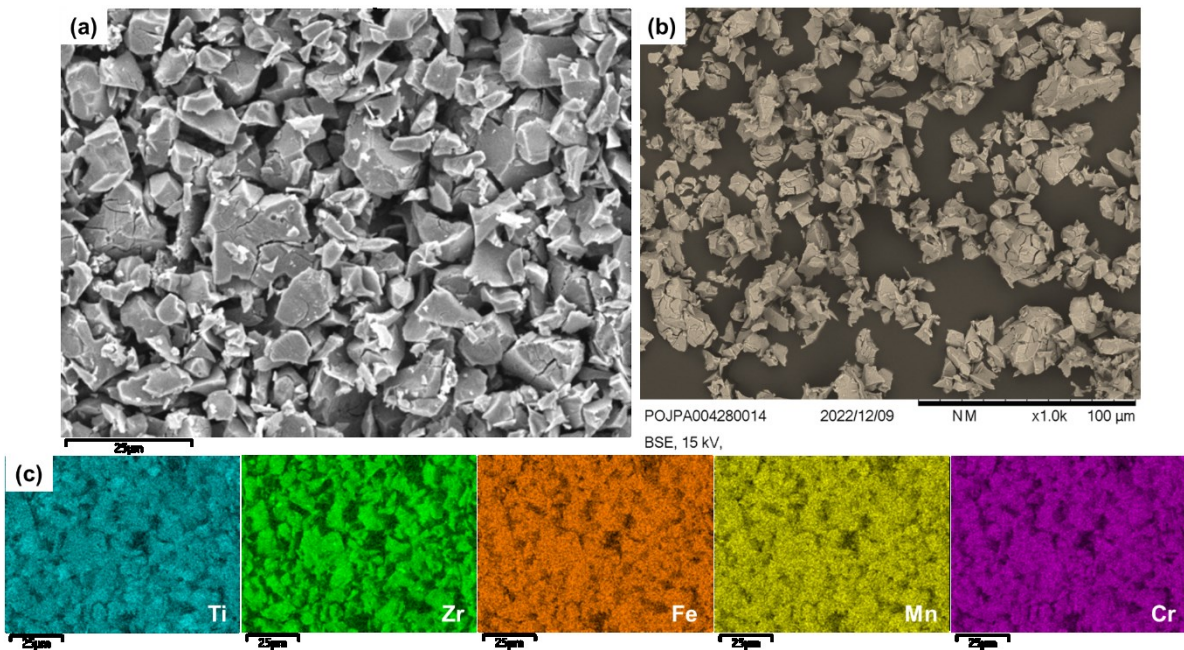


Fig. S6. SEM image and corresponding EDX elemental mappings of the $(\text{Ti}_{0.5}\text{Zr}_{0.5})_1(\text{Fe}_{0.33}\text{Mn}_{0.33}\text{Cr}_{0.33})_2$ alloy after one hydrogenation/dehydrogenation cycle a) and b) SEM images using the Back-Scattered Electrons (BSE) and c) EDS elemental mappings with selected elements: Ti, Zr, Fe, Mn, and Cr.

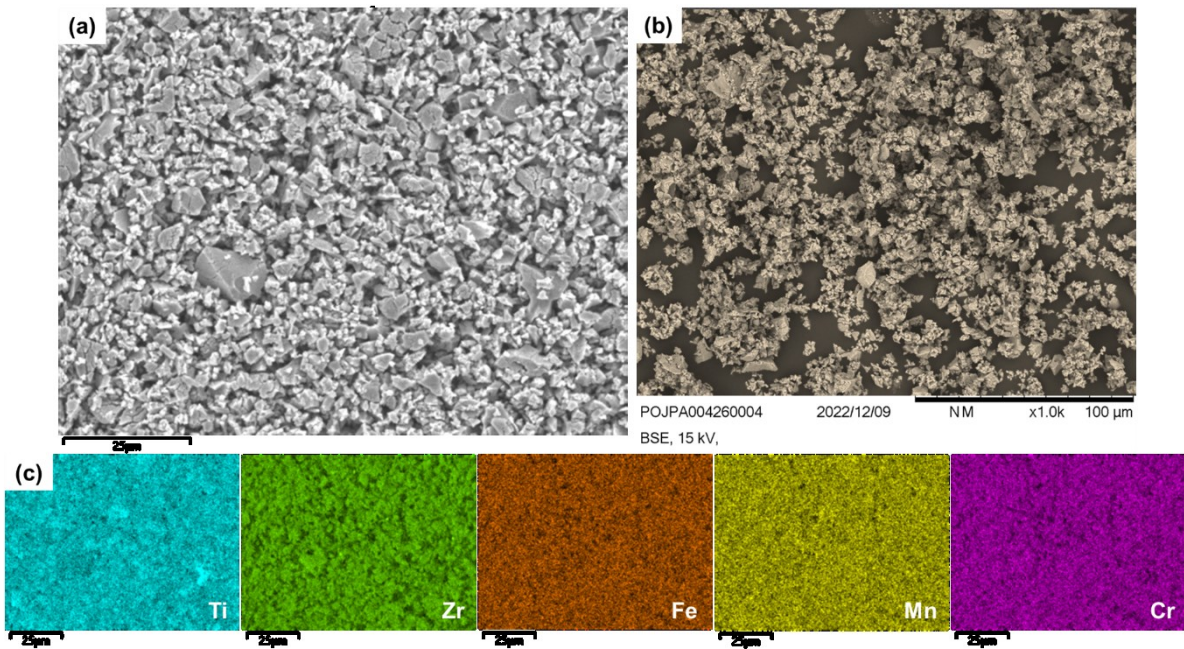


Fig. S7. SEM image and corresponding EDX elemental mappings of the $(\text{Ti}_{0.5}\text{Zr}_{0.5})_1(\text{Fe}_{0.33}\text{Mn}_{0.33}\text{Cr}_{0.33})_2$ alloy after fifty hydrogenation/dehydrogenation cycles a) and b) SEM images using the Back-Scattered Electrons (BSE) and c) EDS elemental mappings with selected elements: Ti, Zr, Fe, Mn, and Cr.

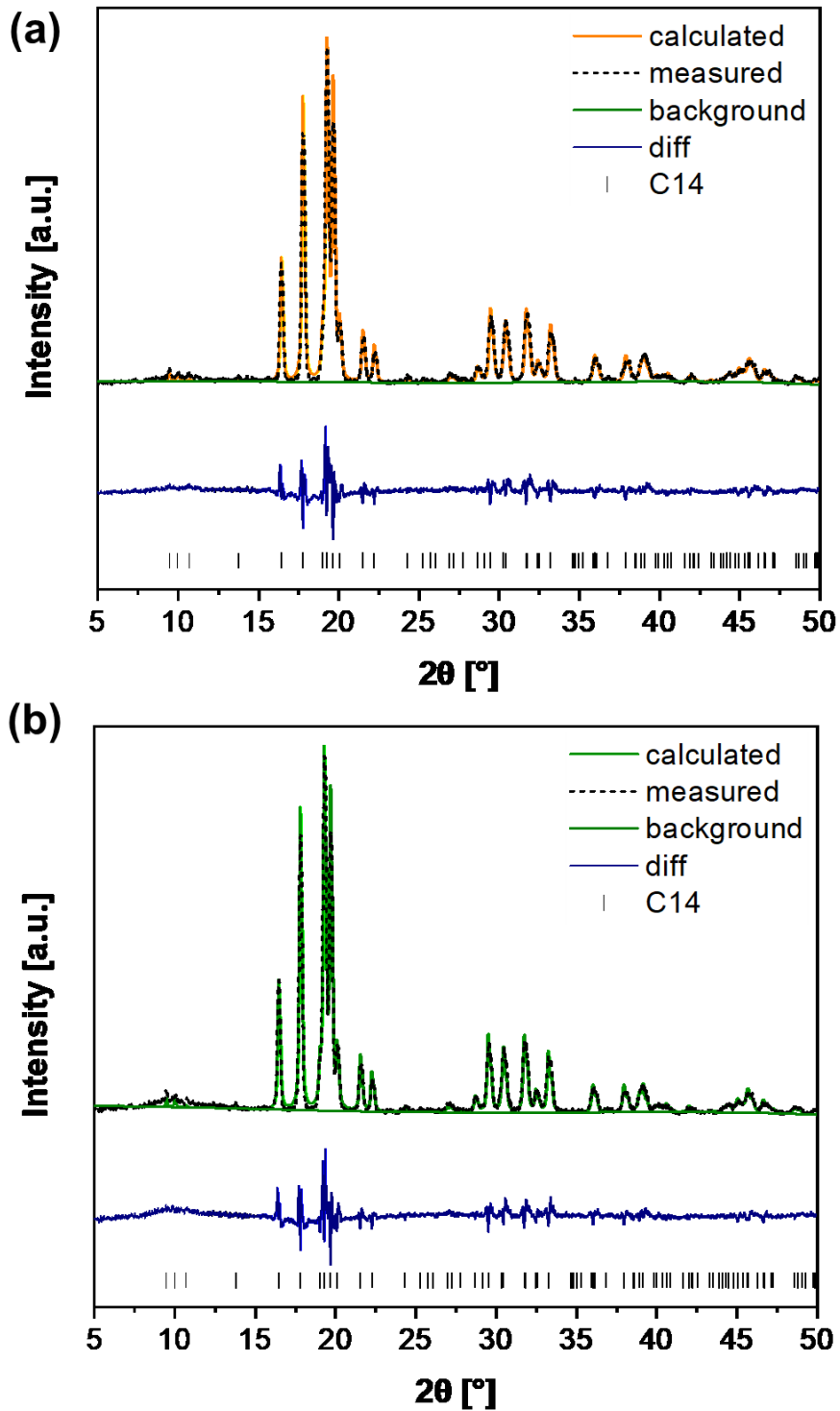


Fig. S8. Rietveld refinement of the XRD pattern of the $(\text{Ti}_{0.5}\text{Zr}_{0.5})_1(\text{Fe}_{0.33}\text{Mn}_{0.33}\text{Cr}_{0.33})_2$ alloy after (a) 1st and (b) 50th cycles of hydrogen absorption and desorption indicating that the sample have C14 Laves phase structure. No reflections from a second phase can be seen.